

Fusion of CT and MRI Images Using OpenCV with FL2440 Hardware

¹N. Sivakumar and ²K. Helenprabha

¹Anna University, Chennai, Tamil Nadu, India

²RMD Engineering College, Chennai, Tamil Nadu, India

Abstract: Multiple acquisition schemes are utilized to acquire complementary informative description associated with an object. Image fusion improve the features of an image (depicting comprehensive description of the object) acquired from different acquisition schemes. The existing homogeneous schemes fail to assign membership to voxels thereby yielding noisy boundaries in the core. In this work, a novel scheme to optimize the kernel is done through class separability criterion using OpenCV tools on hardware (s3c2440a processor) and the algorithms are scalable and generic. PCA based fusion intrinsic dimensionality reduction that uses optimal set of parameters required to account the experiential properties of the data is used. The Bigram Proximity Matrix captures the number of times a feature pair occurs with its columns and rows representing the features of CT and MRI scanned images. The metrics used to evaluate the performance includes MSE, PSNR and Cross entropy. Improved results are achieved with minimum MSE, minimum cross entropy and maximum PSNR.

Key words: Image segmentation, image fusion, OpenCV, kernel optimization, PCA

INTRODUCTION

Image fusion is a process of conjoining corresponding information from several images of the same scene into an image, so that the resulting image contains more accurate depiction of the scene than other individual source images. In this study:

- Multi focus images are combined by using the simple average method in initial phase
- The intermediary fused images are segmented by using the normalized cut method
- Source images are segmented according to the segment output of the intermediate fused image
- Segmented areas of the source images are combined according to their spatial frequencies

Region-based method use the image partitioned into connected regions by grouping neighboring pixels of similar intensity levels. The field of image processing and image fusion has a wide area where image fusion integrates complementary and redundant information from multiple images to create a composite one that contains a better depiction of the scene than other individual source images. Image segmentation is a basic issue in image processing and computer vision. Image segmentation approach is given in Table 1.

Image segmentation: Image segmentation approach and different fusion methods with its description are given in Table 1.

Region-based techniques:

- Provides fast segmentation results by allocating membership to voxels according to homogeneous statistics
- No easier way to distinguish boundaries
- Interior pixels/voxels of the object, method leads to noisy boundaries and creates holes in the interior

Boundary based techniques:

- Attempt to align an initial deformable boundary with the object boundary by reducing the energy functional
- Quantifies the gradient features near the boundary

Fusion method based on segmentation: The region-based fusion method includes:

- Image segmentation
- Wavelet transformation
- Match measure
- Activity measure
- Decision of selecting coefficients
- Coefficients combination
- Inverse wavelet transformation

Table 1: Different fusion methods

Different fusion methods	Description
Average method	Every corresponding pixel is averaged
Max-min intensity method	Resultant pixel = Max [IM(1) pixel, IM(2) pixel]
Wavelet transform	Multi resolution decomposition
Pyramid transform	Forms pyramid at each level of fusion
Multiplicative method	Higher correlation spectral bands are created
Brovery method	Uses arithmetic operations instead of multiplication
Color normalization	Ideal for single sensor fusion
IHS Method	Intensity Hue saturation fusion space is generated from RGB space and intensity match/replace is done
EHLERS Method	Same as HIS but is coupled with a Fourier domain filter
PCA	Creates an uncorrelated feature space

MATERIALS AND METHODS

Earlier work: Lassen *et al.* (2013) presented a watershed transformation based on markers for segmenting the CT image to divide the lungs into lobes. Li *et al.* (2013) proposed a novel vitality framework with descriptor distribution for segmenting the image. Segmenting the target objects from images which has multiple complicated regions, combination of intensity disseminations are corrupted by noise that poses a challenge for the level set models. Li *et al.* (2008) presented the minimization of the energy function is the contour's geodesic length in a flat Riemannian manifold endowed with a metric deduced image features from the boundaries. Comaniciu and Meer (2002) proposed an information fusion method to integrate the information that is extracted from the region based mean shift algorithm with boundary based Canny Edge algorithm into a unified framework. Lanckriet *et al.* (2004) presented an alternate method to optimize the kernel function by maximizing a class separability criterion in the empirical feature space. It develops an effective algorithm to maximize the class separability measure in the empirical feature space. Xiong *et al.* (2005) presented a scheme for optimizing the kernel by maximizing the measure of class separability in the experiential feature space. The kernel is more adaptive on the input that leads to a substantial improvement on the performance for most of the data classification algorithms. Yang *et al.* (2013) presented segmentation of the prostate in magnetic resonance image has become more in need for its assistance to diagnosis and surgical planning of prostate carcinoma. Cristianini *et al.* (2006) presented a novel algorithm to optimize the Gaussian kernel for pattern classification tasks where it have well-separated samples in the kernel feature space. Kafieh *et al.* (2013) proposed a method on vessel segmentation of macular OCT slices on the fundus image using multimodal approach. Wang *et al.* (2005) presented an image fusion method depending on the segmentation region. The images are decomposed into sub-images by wavelet to obtain the segmentation using watershed method for the sub-images that are required to get the regions of each level which is used to guide fusion

process. Morales *et al.* (2013) presented optic disc using automatic detection based on PCA and mathematical morphology that segments the optic disc automatically from a fundus image. Li and Yang (2008) proposed multi-focus image fusion with region segmentation using spatial frequency and simple average and normalized cut method. Bai *et al.* (2013) proposed a multi-atlas method for cardiac Magnetic Resonance (MR) image segmentation by two ways, formulates a fusion model using patch-based label in a Bayesian framework and improves the accuracy in image registration by exploiting label information that leads to enhancement of accuracy in segmentation. Xu *et al.* (2011) proposed a new hybrid image segmentation algorithm that assimilates the extracted information from region-based and boundary-based method.

Image fusion methodology with CT and MRI

Computed Tomography (CT): Computed Tomography is the process of imaging a slice of an object that results in a tomogram. This produces a structure of 2D images in a thin segment of the body by using x-rays.

Magnetic Resonance Imaging (MRI): MRI produces a spatially encoded signal for scanning the body using powerful magnetic fields to polarize and to stimulate the hydrogen nuclei from the water molecules in human tissues. The comparison between CT and MRI is given in Table 2 and the block diagram of image fusion with CT and MRI scan is shown in Fig. 1.

OpenCV tools: OpenCV (open computer vision) provides the basic tools that are essential for solving the problems in computer vision. In some cases, it solves complex problems in computer vision by using the high-level functionalities from the library. Even when this is not the case, the fundamental components in the library are more enough to provide a complete solution in house to almost any computer vision problem. The characteristics of different techniques used for image fusion are given in Table 3.

Table 2: Comparison between CT and MRI

CT	MRI
Poor imaging of soft tissues	Soft-tissues contrast good but dense tissue contrast poor
Safe	Not safe for patients with implanted electrical devices like pacemakers
More comfortable	Less comfortable and patient is placed in a long narrow tube and can be claustrophobic

Table 3: Characteristics of image fusion

Types of IF	Characteristics of fused images			
	Time	Modality	View point	Sensors
Multi-view fusion	Same	Same	Different	Same
Multi-modal	Different	X	Same	Different
Multi-temporal	Different	X	X	X
Multi-focus (focal length various)	Different	X	Different	Same

Table 4: Image acquisition and display on LCD

Title	Description
OpenCV APIs used	The camera captures the image and stores it in buffer. The image in buffer is converted to Mat image. First an empty image is created by using the class Mat To convert the buffer image to Mat image, Mat constructor is used Syntax: Mat: Mat(int rows, int cols, int type, void*data, size_t step = AUTO_STEP) e.g., Mat A(image_height, image_width, CV_8UC2, buf); The Mat image will be in BGR565 format cvtColor()-converts an image from one color space to another e.g., cvtColor(A, frame, CV_BGR5652BGR) The captured image should be displayed on LCD. To display the image, again it should be converted to BGR565 format by using cvtColor(). Then the converted image should be copied to framebuffer device by using Mat: at Syntax: Mat.at<datatype>(row, col) returns pointer to image location e.g., img.at< u16>(y, x)

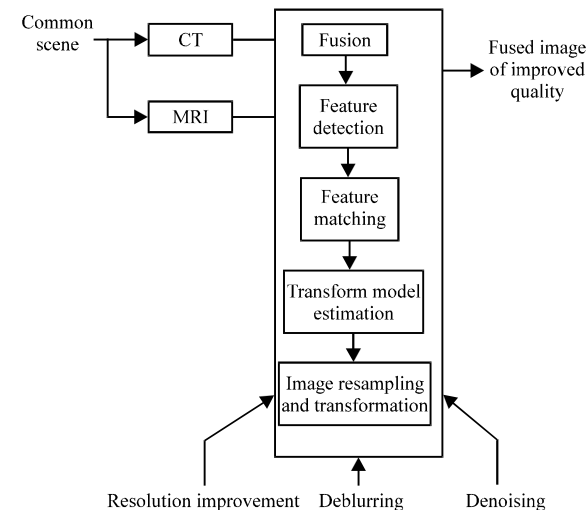


Fig. 1: Block diagram of image fusion with CT and MRI scan

OpenCV based image fusion and image acquisition process: The openCV tools used in this work to perform image acquisition is listed in Table 4.

Image enhancement: The details of OpenCV APIs used to form image enhancement are given in Table 5.

Table 5: OpenCV APIs used to form image enhancement

Title	Description
Create an empty images using class Mat	Mat: A class for creating and storing images e.g., Mat img
To read the images in the folder, imread() is used	Imread: Loads an image from a file. Syntax: Mat imread (const string and filename) e.g., imread (path)
To erode image, erode() is used	Erode: The image will be eroded by using specific structuring element. e.g., erode (img, erode_img, Mat(), Point (-1, -1), value, BORDER_CONSTANT, morphologyDefaultBorderValue())
To dilate image, dilate() is used	Dilate –the image will be dilated by structuring a specific element e.g., dilate (img, dilate_img, Mat(), Point (-1, -1), value, BORDER_CONSTANT, morphologyDefaultBorderValue())
To smoothen the image, GaussianBlur() is used	GaussianBlur: Gaussian filter is used to blur an image e.g., GaussianBlur (img, blur_img, Size (3, 3), value)
To invert image, bitwise_not() is used	bitwise_not: Inverts every bit of an array e.g., bitwise_not(lcd_img, img1)
To adjust brightness of an image add some constant(Scalar value) to each and every pixel of the original image	e.g., bright_img = img + Scalar::all(value)
To contrast image, convertTo() is used	ConvertTo: used to convert an array of one data type to another data type with scaling as an optional e.g., img.convertTo(contrast_img, -1, value, 0)
To add noise to the image, first create an empty matrix with normally distributed random numbers (i.e., noise) using randn()	Randn: used to fill the array with random numbers that are normally distributed e.g., randn(noise, Scalar::all(0), Scalar::all(30))
Now add the created noise to source image using add()	Add: Calculates the sum of two arrays per-element and a scalar e.g., add(lcd_img, noise, noise_img)
To remove noise from the noised image, subtract() is used	Subtract: Calculates the difference between two arrays per-element and a scalar

PCA based fusion intrinsic dimensionality

Proposed method: Figure 2 shows the PCA based fusion intrinsic dimensionality as “the minimum number of parameters needed to account for the observed properties of the data.” Several approaches to estimating the intrinsic dimensionality of a data set is proposed. In this research, an algorithm where the data are divided into small sub-regions and the eigenvalue of the local covariance matrix are computed for each region. The intrinsic dimensionality is then defined based on the size of the eigenvalue and an algorithm for estimating intrinsic dimensionality based on nearest neighbor information and

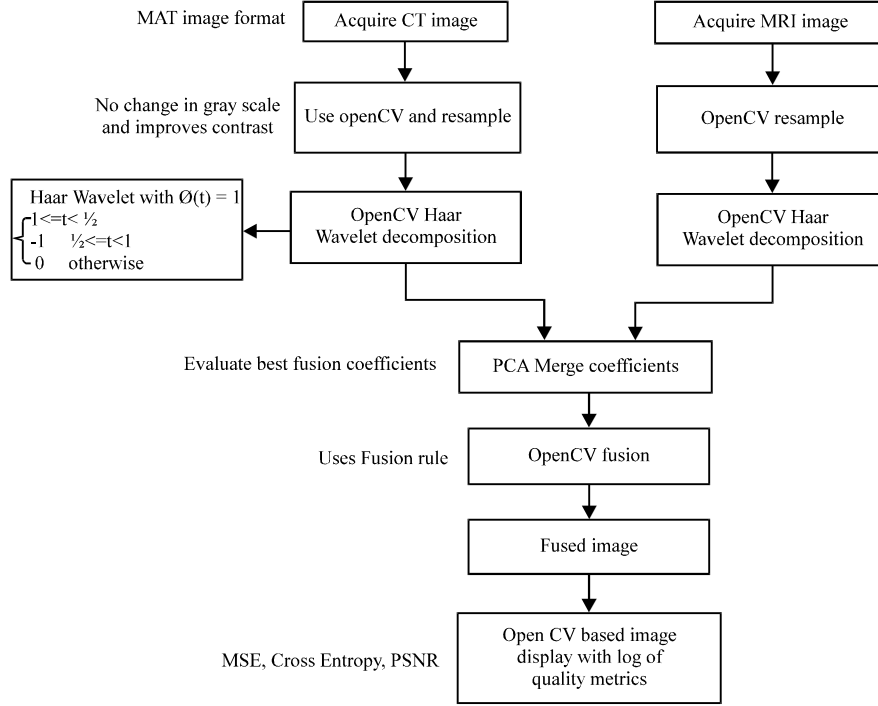


Fig. 2: Proposed method of CT and MRI image fusion

a density estimator is proposed. This method works with the distance between observations, so, it easily extends to the multi-dimensional case. Let, $r_{k, x}$ represent the distance from 'x' to the kth nearest neighbor of 'x' is given (Eq. 1):

$$\bar{r}_k = \frac{1}{n} \sum_{i=1}^n r_{k, x_i} \quad (1)$$

The expected value of the average distance is given in Eq. 2:

$$E(\bar{r}_k) = \frac{1}{G_{k, d}} k^{1/d} C_n \quad (2)$$

where, C_n is independent of 'k'. After rearranging:

$$\log(G_{k, d}) + \log E(\bar{r}_k) = (1/d) \log(k) + \log(C_n) \quad (3)$$

An estimation for $E(\bar{r}_k)$ by taking the observed value of \bar{r}_k based on the sample, yield the following estimator 'd' for the intrinsic dimensionality d:

$$\log(G_{k, d}) + \log(\bar{r}_k) = (1/d) \log(k) + \log(C_n) \quad (4)$$

The slope = $(1/d)$ and $\log(C_n)$ affects the intercept (not the slope) and can be disregarded in the estimation process. A measure of the maximum average distance (to remove outliers) is given by:

$$m_{\max} = \frac{1}{n} \sum_{i=1}^n r_{k, x_i}$$

where, $r_{k, x}$ represents the ith K nearest neighbor distance. Similarly, measure of the spread is given by:

$$S^2_{\max} = \frac{1}{n-1} \sum_{i=1}^n (r_{k, x_i} - m_{\max})^2$$

The data points x_i is used in the nearest neighbor estimate of intrinsic dimensionality as in Eq. 5:

$$r_{k, x_i} \leq m_{\max} + s_{\max} \quad (5)$$

Procedure-PCA based fusion intrinsic dimensionality:
The PCA based fusion intrinsic dimensionality steps are:

- Set $K = k_{\max}$ (a maximum number of the nearest neighbor K)
- Determine all of the r_{k, x_i}
- Remove outliers using (Eq. 5)
- Calculate $\log(\bar{r}_k)$
- Get the initial estimate d_0 by fitting a line to and taking the inverse of the slope
- Calculate $\log(G_{k, d_j})$ using (Eq. 4)
- Update the estimate of intrinsic dimensionality by fitting a line to $\log(G_{k, d_j}) + \log(\bar{r}_k) = (1/d) \log(k)$
- Repeat steps 6 and 7 until convergence condition

PCA using the sample covariance matrix: For the normalized data (i.e., mean = 0) 'X', the sample covariance matrix is defined as:

$$S = (1/(n-1)) X^T_c X_c$$

The jk -th element of S given as:

$$S_{jk} = \frac{1}{n-1} \sum_{i=1}^n (x_{ij} - \bar{x}_j) (x_{ik} - \bar{x}_k) \quad j, k = 1, \dots, p$$

with \bar{x}_j represents the average of x_{ij} . The eigenvectors and eigenvalues of the matrix 'S' can be calculated using Eq. 6 for each j , $j = 1, \dots, p$:

$$|S - \lambda I| = 0 \quad (6)$$

where, I is a $p \times p$ identity matrix and $|\cdot|$ the determinants. The eigenvectors obtained by solving set of Eq. 6 for a_j :

$$(S - \lambda_j I) a_j = 0 \quad j = 1, \dots, p$$

The magnitude of each eigenvector or thogonal to each other is given as:

$$a_i a_i^T = 1, a_i a_j^T = 0$$

for $i, j = 1, \dots, p$ and $i \neq j$. The PCA procedure defines a principle axis rotation of the original variables about their means and elements of the eigenvectors 'a' are the direction cosines that relate the two coordinate systems. Scaling the eigenvector to have unit length produces PCs that are uncorrelated and whose variances are equal to the corresponding eigenvalues such as:

$$v_j = \sqrt{\lambda_j} a_j$$

And:

$$w_j = a_j / \sqrt{\lambda_j}$$

where, a_j are typically needed for hypothesis testing and other diagnostic methods, vector v_j are useful at times, because PCs have the same unit original variables and w_j in the transformation yield PCs are uncorrelated with unit variance. The PC coordinate system via (Eq. 7):

$$Z = X_c A \quad (7)$$

The matrix Z contains the PC scores that have zero mean and are uncorrelated, X transform the observation by similar transformations to get an expression related to the original variables of the PCs which is given by Eq. 8:

$$x = x' + Az$$

The dimensionality reduction with PCA, include in the analysis (those PCs have the highest eigenvalues), thus, the highest amount of variation with fewer dimensions (PC variables) reduce the dimensionality to 'd' as given in Eq. 9:

$$Z_d = X_c A_d \quad (8)$$

where, A_d contains the eigenvectors or column of A , Z_d is an $n \times d$ matrix and A_d is a $p \times d$ matrix.

Feature extraction: The different operations on CT and MRI along with its effects are shown in Table 6.

Bigram proximity matrix mapping: The Bigram Proximity Matrix (BPM) (non-symmetric) captures the number of times feature pair occurs. It is a square matrix whose column and row heading are the features of CT and MRI scanned images. The BPM encoding determines whether or not the representation preserve enough of the semantic content to make separate from BPMs of other thematically unrelated collections of images. The BPM of CT and MRI is given in Table 7 and 8, respectively. Thus, more feature pairs exist in CT (desirable) compared to MRI.

Table 6: Different operations on CT and MRI (sample 1 and 2)





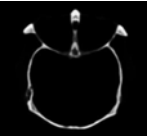
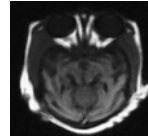
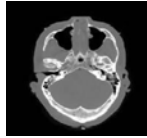
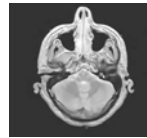
Type of operation	Sample image 1 CT	Sample image 1 MRI	Sample image 2 CT	Sample image 2 MRI
Contour				
Despeck				

Table 6: Continue

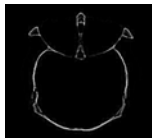
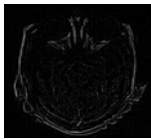
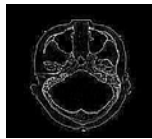


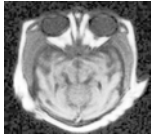
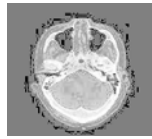
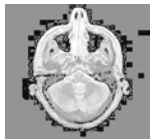
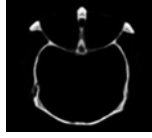
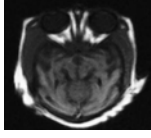
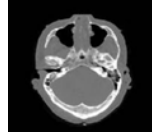
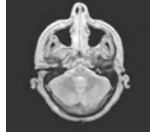






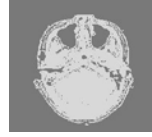



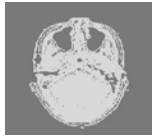

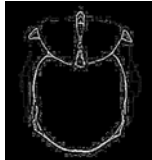

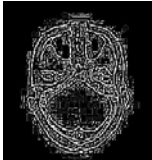
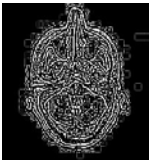
Type of operation	Sample image 1 CT	Sample image 1 MRI	Sample image 2 CT	Sample image 2 MRI
Edge detection				
Equalizer				
Noise				
ROI (region of interest)				
SEG120				
Segment 4				
Spread 2				

Table 7: BPM of CT image (sample 1) with its features

Type of operation	Contour	Despeck	Edge detection	Equalizer	Noise	ROI	SEG120	Segment 4	Spread 2
Contour	1		1						
Despeck		1							
Edge detection			1						
Equalizer				1					
Noise					1				
ROI						1			
SEG120							1		
Segment 4								1	
Spread 2									1

Table 8: BPM of MRI image (sample 1) with its features

Type of operation	Contour	Despeck	Edge detection	Equalizer	Noise	ROI	SEG120	Segment 4	Spread 2
Contour	1								
Despeck		1							
Edge detection			1						
Equalizer				1					
Noise					1				
ROI						1			
SEG120							1		
Segment4								1	
Spread2									1

RESULTS AND DISCUSSION

Hardware implementation results: The metrics used to evaluate the performance of each image is obtained and includes MSE, PSNR and cross entropy. For improved results, MSE and cross entropy should be minimum while PSNR should be maximum. The values are tabulated in Table 9-12. The hardware output on FL2440 board along with the fused images for case (1, 2) is shown in Fig. 3-9.

Table 9: PCA coefficients for image sample 1

Measurements	Expected values	
$C = 1.0e+004^*$	0.8166	0.8440
	0.8440	1.3214
Vector =	-0.8020	0.5973
	0.5973	0.8020
Dvalue = $1.0e+004^*$	0.1880	0
	0	1.9499
PCA =	0.4268	0.5732

Table 10: Output measurement from captured fusion images for sample 2

Measurements	Expected values	
$C = 1.0e+003^*$	1.4959	0.7646
	0.7646	6.1992
Vector =	-0.9877	0.1565
	0.1565	0.9877
Dvalue = $1.0e+003^*$	1.3747	0
	0	6.3203
PCA =	0.1368	
	0.8632	

Table 11: Tabulated values for MSE, PSNR and cross entropy (case 1)

Images	MSE	PSNR	Entropy
CT	5.0543E+03	11.0942	4.4724
MRI	1.0686E+04	7.8425	4.8564
Fused	10.7496	37.8169	1.4261

Table 12: Tabulated values for MSE, PSNR and cross entropy (case 2)

Images	MSE	PSNR	Entropy
CT	271.3063	23.7962	1.9613
MRI	3.3837E+03	12.8368	6.6384
Fused	8.1567	39.0157	1.7767

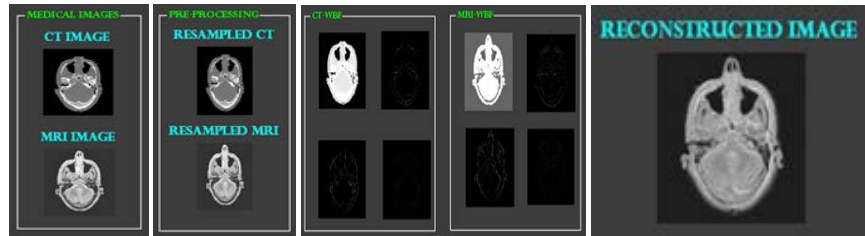


Fig. 3: Sample image 1

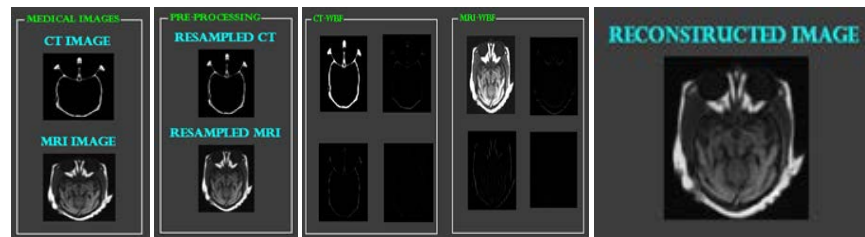


Fig. 4: Sample image 2



Fig. 5: CT and MRI images for sample 1



Fig. 6: CT and MRI images for sample 2

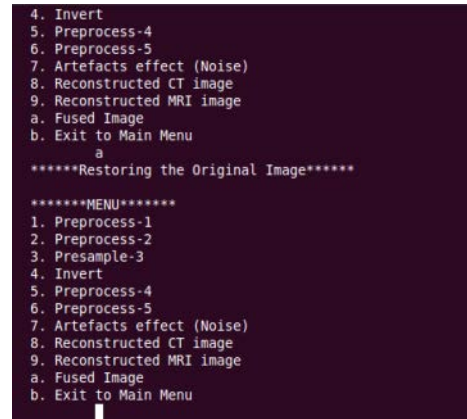


Fig. 9: Hardware based original image

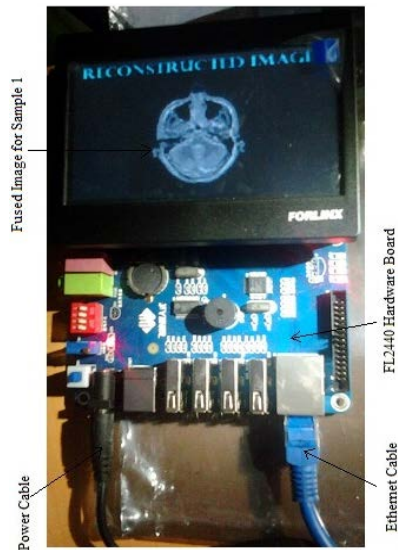


Fig. 7: Fused images for sample 1

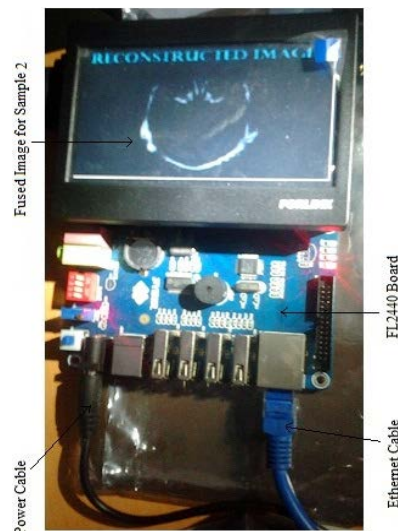


Fig. 8: Fused images for sample 2

CONCLUSION

The quantitative and qualitative mixed fusion scheme proposed in this work provides improved entropy and PSNR and minimum MSE value. The work is more suited when acquired medical image contrast is not good. The hardware implementation makes it suitable for integration in hand held devices. Future direction of study shall focus on implementing all of the transformation functions in the hardware that results in capturing and fusing the images in the handheld devices.

REFERENCES

- Bai, W., W. Shi, D.P. Oregan, T. Tong and H. Wang *et al.*, 2013. A probabilistic patch-based label fusion model for multi-atlas segmentation with registration refinement: Application to cardiac MR images Med. Imaging IEEE. Trans., 32: 1302-1315.
- Comaniciu, D. and P. Meer, 2002. Mean shift: A robust approach toward feature space analysis. IEEE Trans. Patt. Anal. Machine Intel., 24: 603-619.
- Cristianini, N., J. Kandola, A. Elisseeff and J.S. Taylor, 2006. On Kernel Target Alignment. In: Innovations in Machine Learning. Holmes D.E. and L.C. Jain (Eds.). Springer Berlin Heidelberg, Berlin, Germany, ISBN: 978-3-540-30609-2, pp: 205-256.
- Kafieh, R., H. Rabbani, F. Hajizadeh and M. Ommani, 2013. An accurate multimodal 3-D vessel segmentation method based on brightness variations on OCT layers and curvelet domain fundus image analysis. Biomed. Eng. IEEE. Trans., 60: 2815-2823.
- Lanckriet, G.R., N. Cristianini, P. Bartlett, L.E. Ghaoui and M.I. Jordan, 2004. Learning the kernel matrix with semidefinite programming. J. Mach. Learn. Res., 5: 27-72.

- Lassen, B., E.M.V. Rikxoort, M. Schmidt, S. Kerkstra and B.V. Ginneken *et al.*, 2013. Automatic segmentation of the pulmonary lobes from chest CT scans based on fissures, vessels and bronchi. *Med. Imaging IEEE. Trans.*, 32: 210-222.
- Li, C., C.Y. Kao, J.C. Gore and Z. Ding, 2008. Minimization of region-scalable fitting energy for image segmentation. *IEEE Trans. Image Process*, 17: 1940-1949.
- Li, C., X. Wang, S. Eberl, M. Fulham and D. Feng, 2013. A new energy framework with distribution descriptors for image segmentation. *Image Process. IEEE. Trans.*, 22: 3578-3590.
- Li, S. and B. Yang, 2008. Multifocus image fusion using region segmentation and spatial frequency. *Image Vision Comput.*, 26: 971-979.
- Morales, S., V. Naranjo, J. Angulo and M. Alcaniz, 2013. Automatic detection of optic disc based on PCA and mathematical morphology. *Med. Imaging IEEE. Trans.*, 32: 786-796.
- Wang, R., L.Q. Gao, S. Yang, Y.H. Chai and Y.C. Liu, 2005. An image fusion approach based on segmentation region. *Int. J. Inf. Technol.*, 11: 479-486.
- Xiong, H., M.N.S. Swamy and M.O. Ahmad, 2005. Optimizing the kernel in the empirical feature space. *IEEE Trans. Neural Networks*, 16: 460-474.
- Xu, W., R. Kanawong, Y. Duan and G. Zhang, 2011. A new information fusion approach for image segmentation. *Proceedings of the 2011, 18th IEEE International Conference on Image Processing (ICIP)*, September 11-14, 2011, IEEE, Brussels, ISBN: 978-1-4577-1304-0, pp: 2873-2876.
- Yang, M., X. Li, B. Turkbey, P.L. Choyke and P. Yan, 2013. Prostate segmentation in MR images using discriminant boundary features. *Biomed. Eng. IEEE. Trans.*, 60: 479-488.